Supplemental material

Kendrick et al., https://doi.org/10.1083/jcb.201812170

Provided online is one table in Excel. Table S1 provides a list of all proteins that were identified in the KIF1C-BioID and BioID experiments described in Fig. 1. The spectral count (SC) and distributed normalized spectral count abundance factor (dNSAF) are reported for each protein.

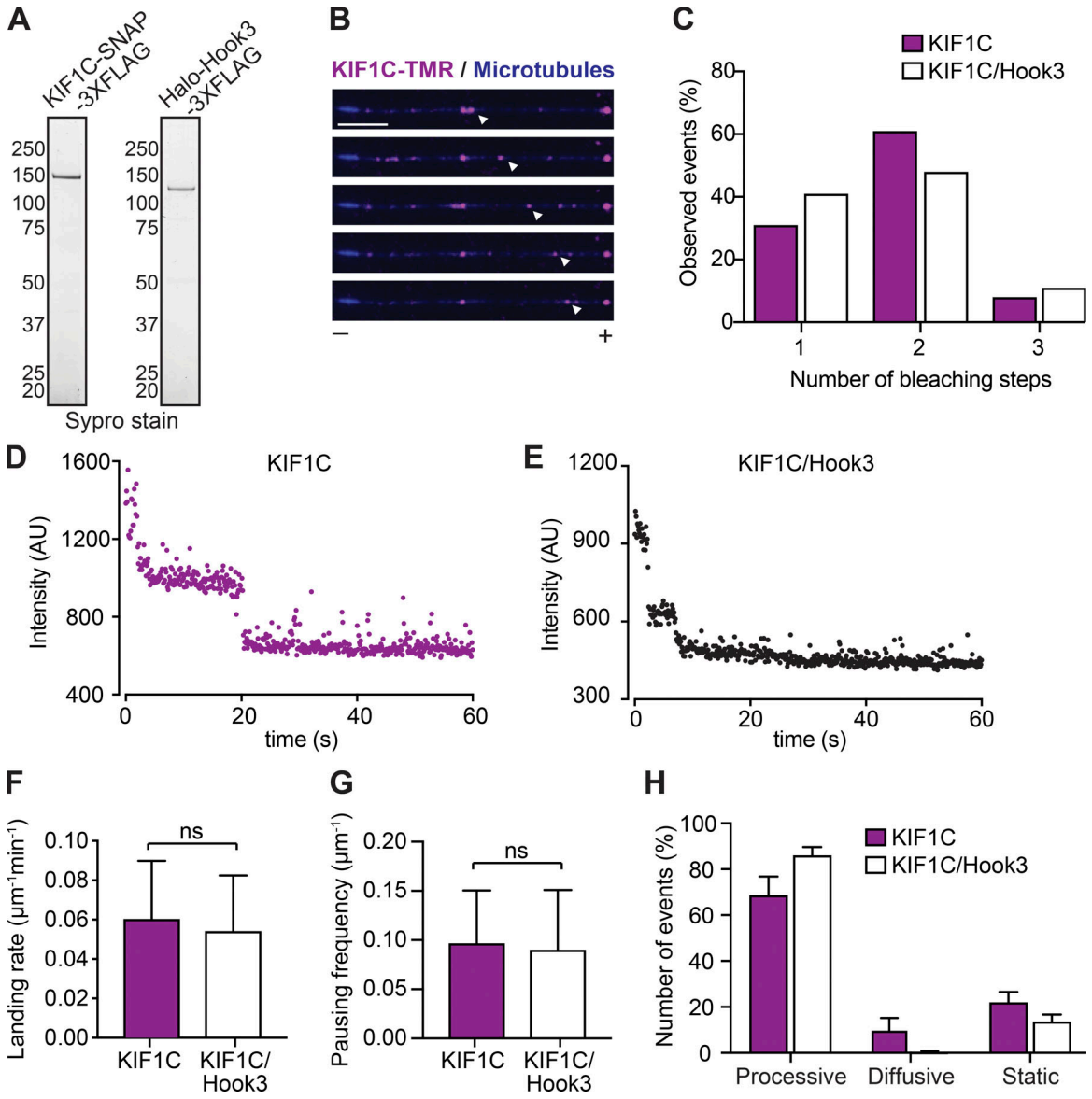

Figure S1. **KIF1C is a processive motor whose motility is not actviated by Hook3. (A)** SDS-PAGE of purified KIF1C-SNAP-3xFLAG and Halo-Hook3-3xFLAG used for motility assays. **(B)** KIF1C-TMR (magenta) motility on polarity marked microtubules. The blue seed made with GMP-CPP tubulin marks the microtubule minus end. Scale bar, 2 µm. White arrows point to a moving KIF1C motor. **(C)** The number of photobleaching steps on microtubules for KIF1C-TMR–only or KIF1C-TMR with Hook3-488 in the presence of AMP-PNP. KIF1C, *n* = 100; KIF1C + Hook3, *n* = 102. Representative data from two independent experiments is shown. **(D)** Example of a two-step photobleaching event for KIF1C. **(E)** Example of a two-step photobleaching event for KIF1C in the presence of Hook3. **(F)** Landing rate (mean ± SD; *n* = 27 for KIF1C, *n* = 64 for KIF1C + Hook3) from KIF1C-TMR–only runs compared with KIF1C-TMR runs collected in the presence of Hook3-488. Statistical significance was calculated using an unpaired *t* test with Welch's correction. Representative data from three independent experiments are shown. ns, not significant. **(G)** Pausing frequency (mean ± SD, *n* = 130 for KIF1C, *n* = 175 for KIF1C + Hook3) from KIF1C-TMR–only runs compared with KIF1C-TMR runs collected in the presence of Hook3-488. Statistical significance was calculated using an unpaired *t* test with Welch's correction. Representative data from three independent experiments are shown. **(H)** Percentage of processive, diffusive, and static events ± SEM in KIF1C-TMR–only runs compared with KIF1C-TMR runs collected in the presence of Hook3-488. Combined data from three independent experiments is shown.

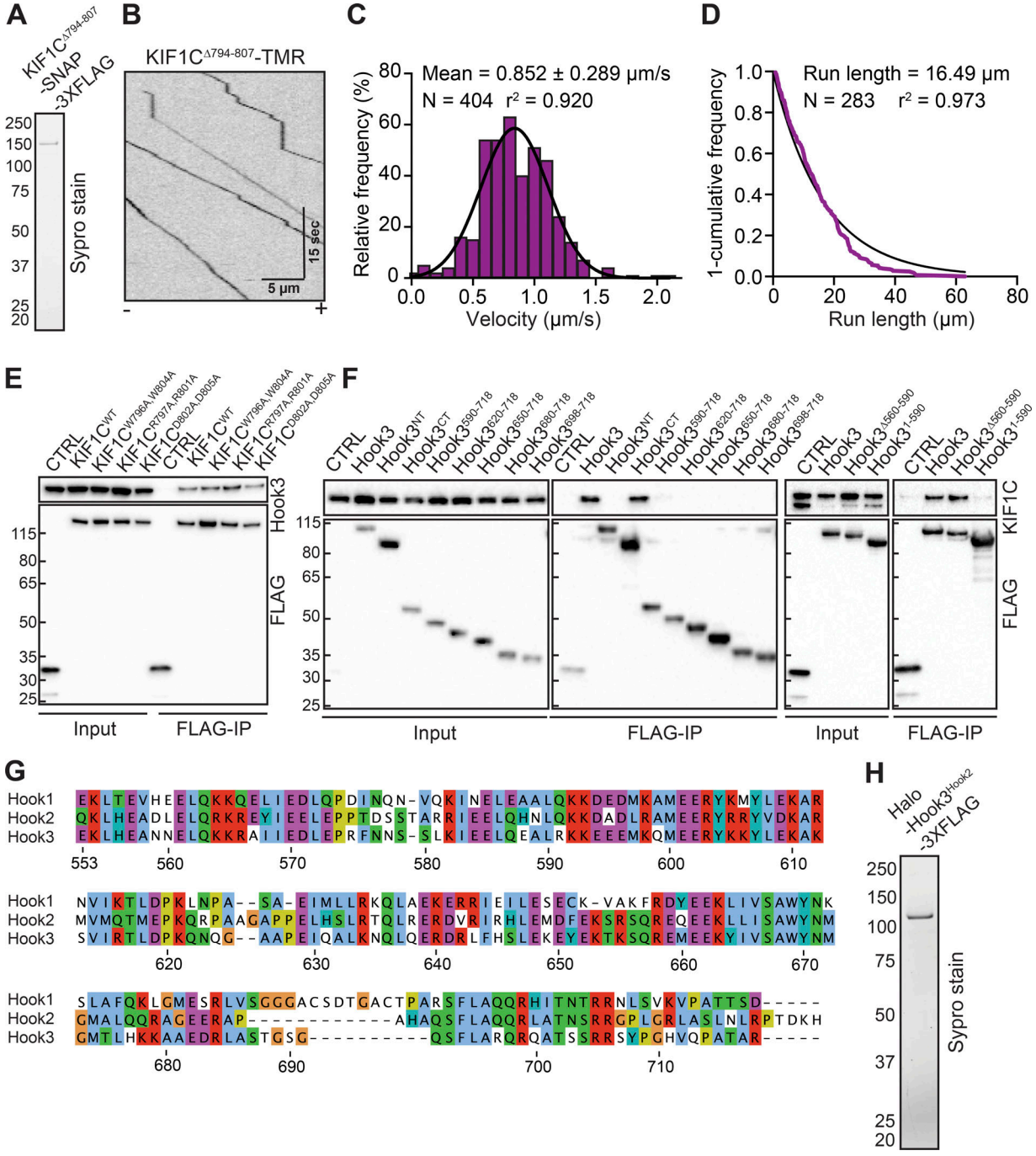

Figure S2. **Mapping of the Hook3 and KIF1C interaction sites. (A)** SDS-PAGE of purified KIF1C$^{\Delta 794\text{-}807}$-SNAP-3xFLAG used for motility assays. **(B)** Representative kymograph from single-molecule motility assays with purified full-length KIF1C$^{\Delta 794\text{-}807}$-SNAP-3xFLAG labeled with TMR. Microtubule polarity is marked with minus (–) and plus (+). **(C)** Single-molecule velocity of KIF1C$^{\Delta 794\text{-}807}$-TMR. A Gaussian fit (black line) to the data from three independent experiments is shown. **(D)** Run length analysis of KIF1C$^{\Delta 794\text{-}807}$-TMR. The 1-cumulative frequency distribution (magenta line) was fit to a one-phase exponential decay (black line). Representative mean decay constant (run length) from three independent experiments is reported. **(E)** Indicated KIF1C-3xFLAG constructs were transiently expressed in 293T cells and immunoprecipitated with FLAG affinity resin (FLAG-IP). Immunoblots were performed with anti-Hook3 and anti-FLAG antibodies. 3xFLAG-sfGFP provided a control (CTRL). Protein molecular weight markers are shown in kilodaltons on the anti-FLAG immunoblot. **(F)** Indicated HaloTag-Hook3-3xFLAG constructs were transiently expressed in 293T cells and immunoprecipitated with FLAG affinity resin (FLAG-IP). Immunoblots were performed with anti-KIF1C and anti-FLAG antibodies. 3xFLAG-sfGFP provided a control. Protein molecular weight markers are shown in kilodaltons on anti-FLAG immunoblots. **(G)** Sequence alignment of the carboxy-terminal regions of the three human hook homologues (Hook3, aa 552–718, Hook2, aa 548–719, and Hook1, aa 556–728) made using Clustal Omega. **(H)** SDS-PAGE of purified Halo tagged Hook3^{Hook2}-3xFLAG used for motility assays.

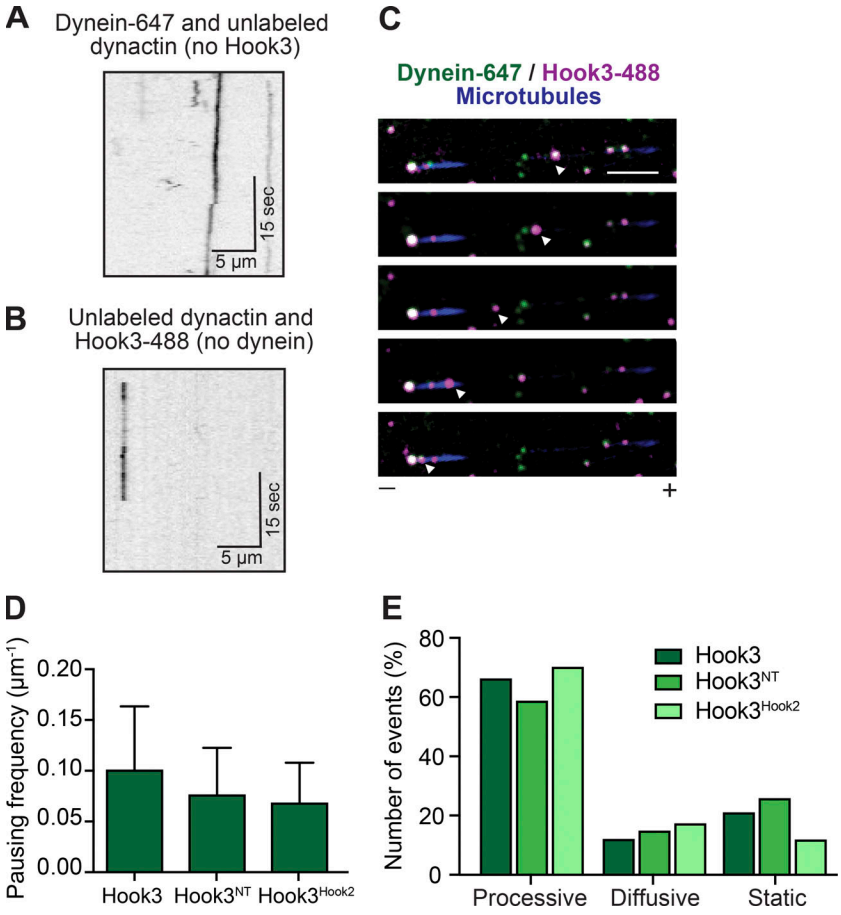

Figure S3. **Purified full-length Hook3, the Hook3 amino terminus, and a Hook3-Hook2 chimera activate dynein motility. (A)** Representative kymograph from single-molecule motility assays with dynein-647 and unlabeled dynactin in the absence of Hook3. **(B)** Representative kymograph from single-molecule motility assays with unlabeled dynactin and Hook3-488 in the absence of dynein. **(C)** Dynein-647 (green) motility in the presence of full-length Hook3-488 (magenta) and unlabeled dynactin on polarity marked microtubules. The blue seed made with GMP-CPP tubulin marks the microtubule minus end. Microtubule polarity is marked with minus (–) and plus (+). Scale bar, 2 µm. White arrows point to a moving dynein/dynactin/Hook3 complex. **(D)** Pausing frequency ± SD of dynein/dynactin complexes in the presence of the indicated activating adaptors (Hook3, n = 72; Hook3^{NT}, n = 24; Hook3^{Hook2}, n = 53). Representative data from at least two independent experiments is shown. **(E)** The number of processive, diffusive, and static events for dynein/dynactin complexes in the presence of the indicated activating adaptors. Representative data from at least two independent experiments is shown.

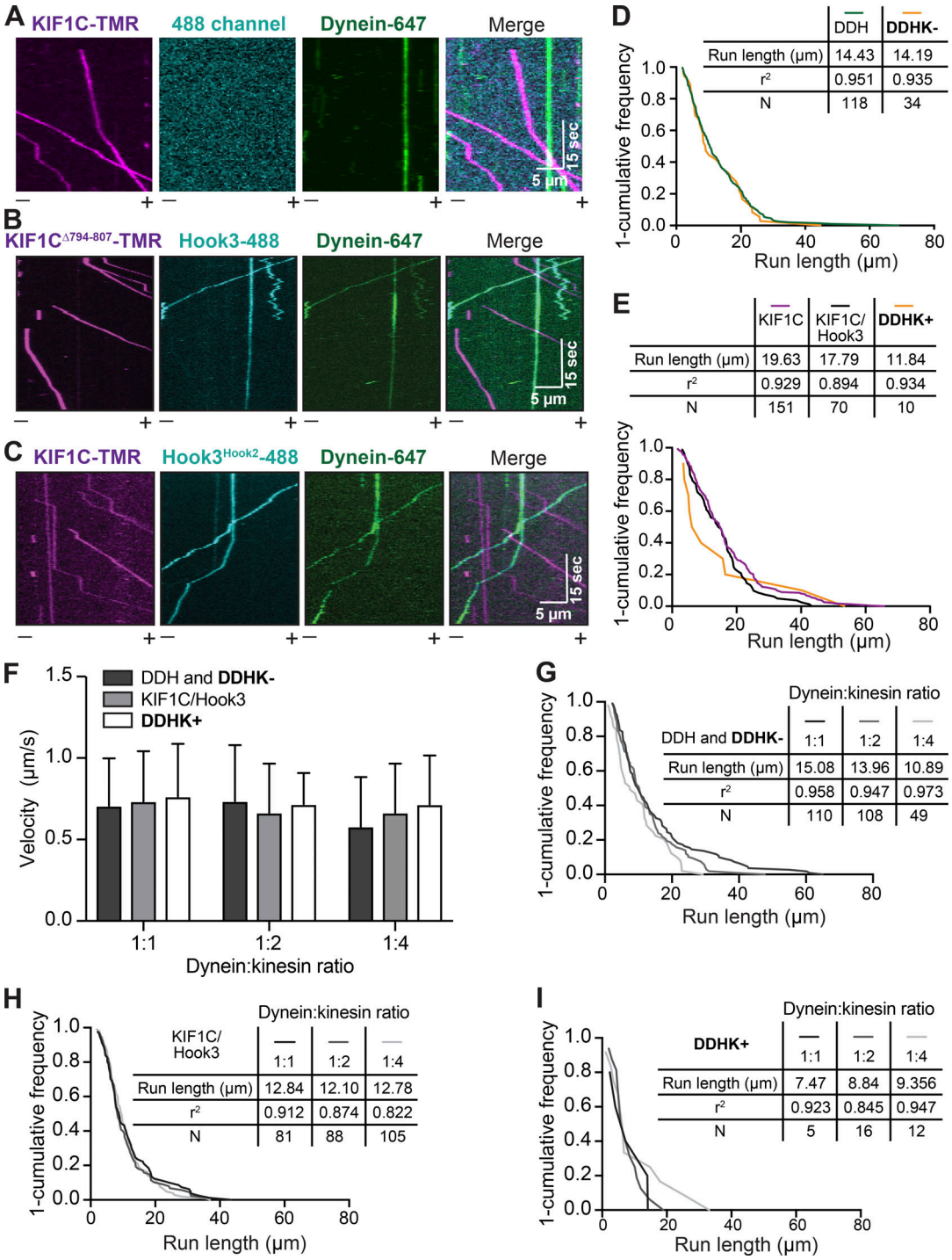

Figure S4. **Hook3 is a scaffold for opposite polarity motors. (A)** Representative kymographs from single-molecule motility assays with purified dynein-647, unlabeled dynactin, and KIF1C-TMR. No Hook3 is present in the sample mixture as represented by the lack of signal in the 488 channel. Microtubule polarity is marked with minus (–) and plus (+). **(B)** Representative kymographs from single-molecule motility assays with purified dynein-647, unlabeled dynactin, KIF1C$^{\Delta 794-807}$-TMR, and Hook3-488. Microtubule polarity is marked with minus (–) and plus (+). **(C)** Representative kymographs from single-molecule motility assays with purified dynein-647, unlabeled dynactin, KIF1C-TMR, and Hook3^{Hook2}-488 chimera. Microtubule polarity is marked with minus (–) and plus (+). **(D)** Run length analysis of all minus end–directed events reported in Fig. 5 D. The 1-cumulative frequency distribution was fit to a one-phase exponential decay (not shown). Mean decay constants (run length) are reported. **(E)** Run length analysis of all plus end–directed events reported in Fig. 5 D. The 1-cumulative frequency distribution was fit to a one-phase exponential decay (not shown). Representative mean decay constants (run length) are reported. Note that the *n* value for DDHK+ is too low for an accurate fit. **(F)** Velocity ± SD of the indicated complexes (1:1 ratio: DDH and DDHK–, *n* = 171; KIF1C/Hook3, *n* = 70; DDHK+, *n* = 9. 1:2 ratio: DDH and DDHK–, *n* = 161; KIF1C/Hook3, *n* = 137; DDHK+, *n* = 22. 1:4 ratio: DDH and DDHK–, *n* = 59; KIF1C/Hook3, *n* = 214; DDHK+, *n* = 22). Combined data from two independent experiments is shown. **(G–I)** Run length analysis of the indicated complexes. The 1-cumulative frequency distribution was fit to a one-phase exponential decay (not shown). Representative mean decay constants (run length) are reported. Note that the *n* value for DDHK+ is too low for an accurate fit.

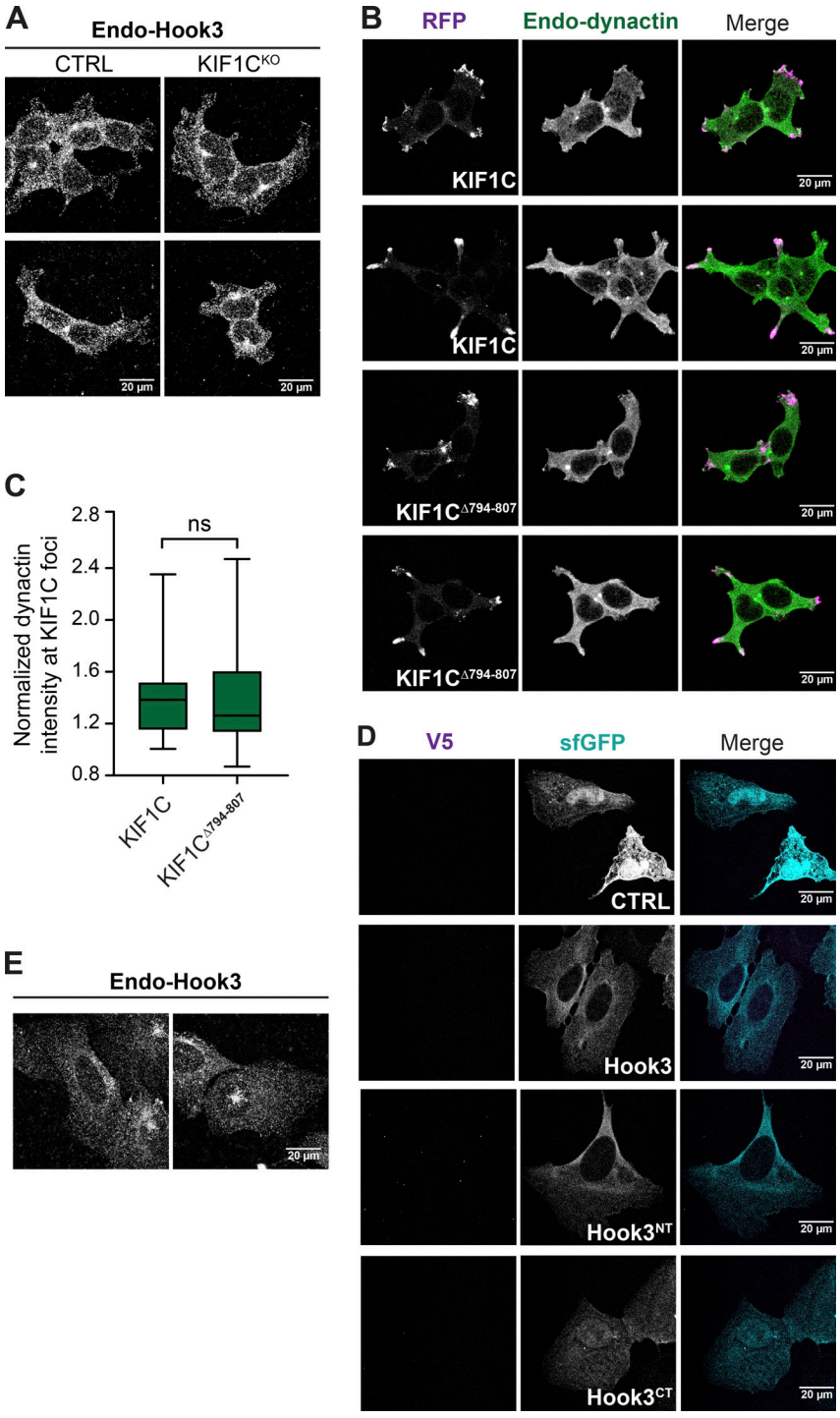

Figure S5. **Dynactin localization is unaffected by KIF1C expression. (A)** Confocal microscopy of endogenous Hook3 in control and KIF1C knockout 293T cells. 293T Cas9 control (CTRL) and KIF1C^{KO} cells were grown on glass coverslips, fixed, and stained for endogenous Hook3 (Endo-Hook3). The Hook3 signal is shown in representative maximum intensity projections. **(B)** Confocal microscopy of KIF1C and dynactin localization in 293T KIF1C-tagRFP-3xFLAG and KIF1C$^{\Delta794\text{-}807}$-tagRFP-3xFLAG stable cell lines. 293T KIF1C tagRFP-3xFLAG or KIF1C$^{\Delta794\text{-}807}$-tagRFP-3xFLAG cells were grown on glass coverslips, fixed, and stained for endogenous dynactin (Endo-dynactin). The tagRFP and dynactin signals are shown in representative maximum intensity projections. **(C)** The mean normalized dynactin intensity within KIF1C foci for cells stably transfected with different KIF1C constructs (KIF1C-tagRFP-3xFLAG, n = 21 or KIF1C$^{\Delta794\text{-}807}$-tagRFP-3xFLAG, n = 26). Foci were determined by thresholding the KIF1C image, and masks of these foci were used to measure the dynactin intensity in these corresponding regions in maximum projection images. Box plots represent maximum and minimum values. Statistical significance was calculated with an unpaired t test. Representative data from three independent experiments is shown. ns, not significant. **(D)** Confocal microscopy of Hook3 in U2OS cells. Cells were grown on glass coverslips and transiently transfected with the indicated sfGFP-tagged Hook3 (full-length Hook3, Hook3^{NT} [aa 1–552], Hook3^{CT} [aa 553–718]), or control sfGFP constructs. 24 h after the transfections, the cells were fixed and stained with a V5 specific antibody. The V5 and sfGFP signals are shown in representative maximum intensity projections. **(E)** Confocal microscopy of endogenous Hook3 in U2OS cells. Cells were grown on glass coverslips, fixed, and stained for endogenous Hook3 (Endo-Hook3). The Hook3 signal is shown in representative maximum intensity projections.

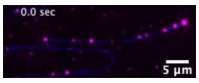

Video 1. **KIF1C motility on microtubules.** KIF1C-TMR (magenta) moving on 405-labeled microtubules (blue). Images were collected using TIRF microscopy. Frames were taken every 400 ms for 180 s. Video frame rate is 24 frames/s. Scale bar, 5 µm.

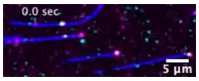

Video 2. **KIF1C motility on microtubules in the presence of Hook3.** KIF1C-TMR (magenta) mixed with Hook3-488 (cyan) moving on 405-labeled microtubules (blue). Images were collected using near-simultaneous TIRF microscopy. Frames were taken every 400 ms for 180 s. Video frame rate is 24 frames/s. Scale bar, 5 µm.

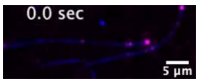

Video 3. **KIF1C$^{\Delta 794\text{-}807}$ motility on microtubules.** KIF1C$^{\Delta 794\text{-}807}$-TMR (magenta) moving on 405-labeled microtubules (blue). Images were collected using TIRF microscopy. Frames were taken every 400 ms for 180 s. Video frame rate is 24 frames/s. Scale bar, 5 µm.

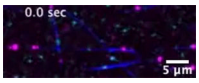

Video 4. **KIF1C$^{\Delta 794\text{-}807}$ motility on microtubules in the presence of Hook3. KIF1C$^{\Delta 794\text{-}807}$-TMR (magenta) mixed with Hook3-488 (cyan) moving on 405-labeled microtubules (blue).** Images were collected using near-simultaneous TIRF microscopy. Frames were taken every 400 ms for 180 s. Video frame rate is 24 frames/s. Scale bar, 5 µm.

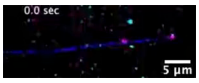

Video 5. **KIF1C motility on microtubules in the presence of Hook3^{Hook2}. KIF1C-TMR (magenta) mixed with Hook3^{Hook2}-488 (cyan) moving on 405-labeled microtubules (blue).** Images were collected using near-simultaneous TIRF microscopy. Frames were taken every 400 ms for 180 s. Video frame rate is 24 frames/s. Scale bar, 5 µm.

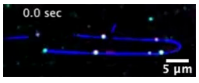

Video 6. **Motility of dynein, dynactin and Hook3 on microtubules.** Dynein-647 (magenta), unlabeled dynactin, and Hook3-488 (cyan) movement on 405-labeled microtubules (blue). Images were collected using near-simultaneous TIRF microscopy. Frames were taken every 400 ms for 180 s. Video frame rate is 24 frames/s. Scale bar, 5 µm.

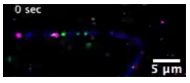

Video 7. **Example of motility of dynein, dynactin, Hook3, and KIF1C on microtubules.** Dynein-647 (green), unlabeled dynactin, Hook3-488, and KIF1C-TMR (magenta) movement on 405-labeled microtubules (blue). Hook3-488 channel was omitted in the merge image for easier viewing. White arrow follows a run colocalized in dynein, Hook3, and KIF1C channels. Images were collected using near-simultaneous three-color TIRF microscopy. Frames were taken every 400 ms for 180 s. Video frame rate is 24 frames/s. Scale bar, 5 µm.

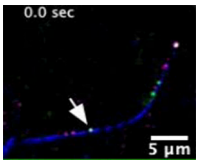

Video 8. **Example of motility of dynein, dynactin, Hook3, and KIF1C on microtubules.** Dynein-647 (green), unlabeled dynactin, Hook3-488, and KIF1C-TMR (magenta) movement on 405-labeled microtubules (blue). Hook3-488 channel was omitted in the merge image for easier viewing. White arrow follows a run colocalized in dynein, Hook3, and KIF1C channels. Images were collected using near-simultaneous three-color TIRF microscopy. Frames were taken every 400 ms for 180 s. Video frame rate is 24 frames/s. Scale bar, 5 µm.